

XEUS wide-field imager: first experimental results with the X-ray active pixel sensor DEPFET

L. Strüder^a, G. Hasinger^a, P. Holl^b, P. Lechner^b, G. Lutz^c, M. Porro^d, R. Richter^c, H. Soltau^b, J. Treis^a

^a Max-Planck-Institut für extraterrestrische Physik, Giessenbachstr., D-85741 Garching, Germany

^b PNSensor GmbH, Römerstr. 28, D-80803 München, Germany

^c Max-Planck-Institut für Physik, Föhringer Ring 6, D-80805 München, Germany

^d Politecnico di Milano, Piazza Leonardo da Vinci 32, I-20133 Milano, Italy

ABSTRACT

A new type of Active Pixel Sensor is proposed which will be capable to meet the requirements of the wide field imager of ESA's future X-ray mission XEUS: the simultaneous energy and position resolved detection of X-rays at high count rate on a large format sensor. The Active Pixel Sensor is based on the integrated detector-amplifier structure DEpleted P-channel Field Effect Transistor (DEPFET). The device operates on a fully depleted bulk and provides internal signal amplification at the position of the charge generation. A very low value of the overall output capacitance leads to extremely low read noise. In the matrix arrangement of an Active Pixel Sensor the single DEPFET pixels can be randomly accessed for readout, and various flexible readout modes are possible. In contrast to CCDs the DEPFET-based Active Pixel Sensor avoids the transfer of signal charges over long distances within the detector bulk, and related problems of transfer loss or out-of-time-events cannot occur. An interesting feature is the non-destructive nature of the DEPFET readout which can be used for the reduction of the low-frequency noise contribution by repetitive readings of the signal information. The device principle of the DEPFET based pixel sensor is explained. First results of single DEPFET measurements are presented.

1. THE XEUS MISSION

The X-ray Evolving Universe Spectroscopy (XEUS) mission is a potential follow-on mission to the XMM-Newton satellite and currently under study within the European Space Agency's (ESA) Horizon 2000+ program. The aim of XEUS is to operate a permanent satellite observatory for the X-ray energy band from 100 eV to 30 keV with a telescope aperture equivalent to the largest ground based optical telescopes, i.e. in the order of 10 m². XEUS will be the first instrument to perform detailed imaging spectroscopic studies of some of the unresolved issues of high-energy astrophysics concerning the early stage of the universe. Among the scientific goals are the study of first massive black holes, the formation of first gravitationally bound galaxy groups and their development towards clustering, and the evolution of chemical element synthesis¹.

The initial mission configuration will consist of a mirror spacecraft (MSC) with an effective area of 6 m² at 1 keV and a separate detector spacecraft (DSC)². The two spacecrafts are aligned by active control at a focal length of 50 m with a relative accuracy of 1 mm³. After several years of operation XEUS will dock to the International Space Station (ISS) where the MSC will be upgraded to an effective area of 30 m² at 1 keV by the robotic mounting of additional mirror segments³. A new detector spacecraft with advanced sensor technology will then replace the DSC. The launch of XEUS will be presumably in 2015. With the potentialities of the ISS for mirror extension, and with the option of detector substitution the mission lifetime may be well over a quarter of a century.

The XEUS focal plane instrumentation will consist of two Narrow Field Imagers (NFIs) and a Wide Field Imager (WFI)⁴. The NFIs will be based on cryogenic imaging spectrometers like superconducting tunnel junctions and transition edge sensors and cover a field of view (FOV) of 1 arcmin, i.e. about 1.5 cm x 1.5 cm at 50 m focal length. With their energy resolution of 1 eV to 10 eV FWHM over the full energy range from 100 eV to 30 keV the NFIs will be able to resolve the fine structure in the X-ray emission of differently ionized atoms. The WFI will work mainly as a pathfinder for the NFIs.

2. THE XEUS WIDE FIELD IMAGER

The wide field imaging detector on XEUS will cover a 5 arcmin field of view (FOV), translating into a total detector area of 7.5 cm x 7.5 cm. To match the telescope's expected spatial resolution of 2 arcsec half energy width (HEW) the pixel size has to be smaller than 100 μm x 100 μm . The WFI's required energy resolution is 50 eV FWHM at the C-K line (277 eV) and 125 eV FWHM at the Mn-K α line (5.9 keV). Compared to the current X-ray satellite missions XMM-Newton and Chandra, the XEUS telescope will bring an enormous increase in sampling area. The throughput will grow by a factor of 25 in the initial XEUS configuration with respect to XMM-Newton, and by a factor of 100 after the mirror upgrade. Developing a detector for the WFI count rate capability has to be one of the major concerns.

CCDs have been the prevailing image sensor technology during the past decades for visible light as well as for X-rays. However, the CCD concept has fundamental handicaps inherent to the need of a close-to-perfect charge transfer over macroscopic distances inside the semiconductor bulk⁷:

- The required high charge transfer efficiency depends on the quality of the bulk material and may deteriorate by radiation damage during the CCD's lifetime. For instance, the frontside illuminated CCDs of the ACIS camera onboard the Chandra satellite have degraded drastically by proton irradiation during radiation belt passages⁸.
- The relatively slow transfer process limits the readout rate.
- The access to the contents of the individual pixels is strictly sequential.
- Out-of-time events, i.e. photons hitting the CCD during the charge transfer cycle, appear at an erroneous position in the image.

For those reasons the semiconductor laboratory of the Max-Planck-Institutes for physics and for extraterrestrial physics started to adapt the concept of the Active Pixel Sensor (APS), which has gained a considerable share in the market of optical digital cameras, to the requirements of X-ray imaging spectroscopy. An APS is defined as a two-dimensional structured detector array with an amplifying element in each pixel. This concept avoids the above mentioned CCD-intrinsic problems. As integrated amplifier the DEpleted P-channel Field Effect Transistor (DEPFET) is introduced in the next section.

3. THE DEPFET CONCEPT

The DEPFET was introduced in 1987^{9, 10} as a derivative of the basic detector principle of sideward depletion¹¹, i.e. the full depletion of a semiconductor volume by reverse biased rectifying junctions covering both surfaces. The DEPFET consists of a p-channel field effect transistor on a high resistivity n-type silicon bulk (fig. 1). The transistor may be either a JFET, or a MOSFET of enhancement or depletion type. The bulk is completely depleted by the reverse biased p+ doped backside diode and by the p+ doped FET contacts source and drain. The voltage applied to the backside diode is high compared to the transistor voltages, so that the distribution of the electron potential energy in a cross section perpendicular to the surface has the shape of a parabola with a minimum close to the upper surface in the depth of about 0.5 μm . An additional deep n-doped region enhances the depth of the potential minimum and confines it in the lateral direction to the extent of the FET channel.

Electron hole pairs released in the depleted volume by thermal generation or by the absorption of ionizing radiation are separated in the electric field of the depletion region. While the holes drift to the back contact, the electrons are accumulated in the potential minimum and enhance the transistor current by inducing additional positive image charges inside the FET channel. Thus the DEPFET's current is a function of the amount of charges in the potential minimum, and its measurement yields information about the energy absorbed in the depleted volume. To express the current steering function of the stored electrons the potential minimum is called 'internal gate'. It has a measured sensitivity of 200 pA per electron¹². The internal gate's geometric size and doping concentration are dimensioned to store more than 10⁵ electrons, enough to perform a reliable discrimination of minimum ionizing particles. Unlike a conventional detector-preamplifier system, the DEPFET is free of interconnection stray capacitance and the overall capacitance is minimized.

The internal gate exists, i.e. electrons are collected and stored in it, regardless of a current flowing in the DEPFET channel or not. The transistor current may be turned off during signal integration and only switched on via the external gate for the signal readout, thus minimizing power consumption. The reset of the device, i.e. the removal of electrons from the internal gate's potential well, is done by periodically applying a positive voltage pulse to an adjacent n⁺ doped 'clear' contact acting as drain for electrons. The clear contact is separated from the detector bulk by a deep p-implanted well (fig. 1).

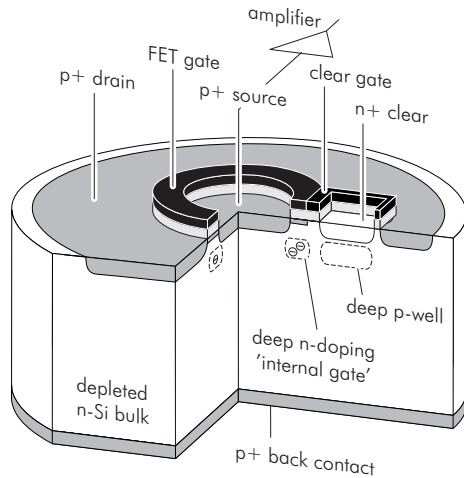


Figure 1

Section of a DEPFET in circular geometry. Electrons generated by the absorption of ionizing radiation drift to the potential minimum of the 'internal gate' and enhance the transistor current by inducing positive image charges inside the FET channel. Applying a positive voltage pulse to the clear contact and to the clear gate resets the device.

The signal information, i.e. the current change proportional to the amount of stored charges, is obtained by a comparative measurement of the DEPFET current with empty and filled internal gate. Due to the DEPFET's charge storage capability it is not necessary to measure the current difference of the two states while the signal charges arrive at the internal gate, but the comparison can be made at any time. The DEPFET may be turned off before, after, and in between both measurements. For noise considerations it is of advantage to keep the time between both measurements as short as possible. This is in contradiction to the standard operation mode of a pixel sensor with a long integration period elapsing

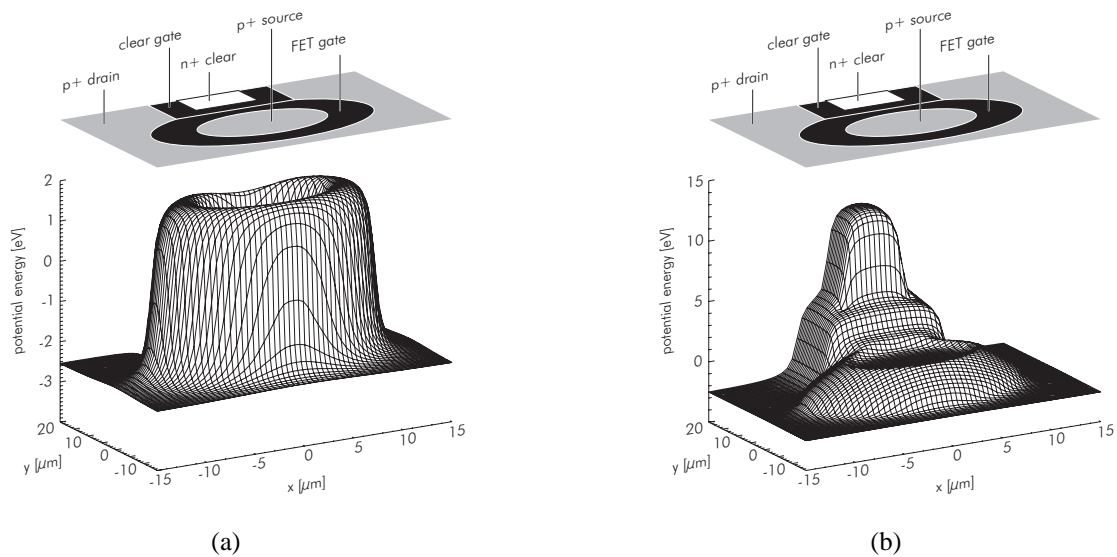


Figure 2

Potential distribution of a circular DEPFET as shown in fig. 1 in a cross section parallel to the surface in a depth of $0.5 \mu\text{m}$, i.e. a horizontal cut through the internal gate, simulated by the 3-D Poisson solver POSEIDON^{14, 15}. In this graphic representation electrons drift uphill. In integration mode (a) the ring-shaped internal gate is the most attractive region for electrons. During the clear pulse (b) stored electrons follow the rising potential to the clear contact.

between the reset and the signal readout. For low noise readout of an APS it is therefore favorable to invert the order of readings following the sequence:

- i. integration of signal charges while the transistor current is switched off,
- ii. switch-on of the DEPFET current via the external gate,
- iii. signal readout with filled internal gate,
- iv. reset by the clear contact,
- v. baseline readout with empty internal gate,
- vi. switch-off of the DEPFET current.

The difference between the current levels measured in steps iii and v yields the signal information. This readout scheme requires a reproducible baseline, and for that reason the complete removal of the signal electrons from the internal gate is mandatory. Otherwise, the undefined number of remaining electrons in the internal gate would cause the problem of kTC or reset noise¹³. To ensure a complete clear the clear contact is surrounded by an additional MOS ‘clear gate’ (fig. 1). Depending on its bias the clear gate acts like an additional drain region or like an extended clear contact. During signal integration and readout, the clear gate is set to a negative voltage to define a potential well that restricts electrons to the internal gate and prevents the injection of electrons from the clear contact to the internal gate. During the reset both clear contact and clear gate are set to a positive voltage. For an efficient reset the clear gate protrudes into the external gate of the FET (fig. 1).

The different working points of a circular DEPFET as shown in fig. 1 have been simulated using the 3D numerical Poisson solver POSEIDON^{14, 15}. Figure 2 shows the resulting electron potential distributions in a plane parallel to the surface at a depth of 0.5 μm , i.e. a section through the internal gate. In this graphic representation of the potential energy electrons drift uphill. The DEPFET is shown in two operating conditions: During charge integration the ring shaped internal gate is the most attractive region. The potential difference to the surrounding drain is more than 3 V and electrons will drift and be stored there (fig. 2a). For the clear procedure both clear contact and clear gate are pulsed in the positive direction (+12 V and +6 V), and the stored electrons have to follow the steadily rising potential to the clear contact (fig. 2b).

Next to the circular DEPFET geometry as shown in figs. 1 and 2 with concentric source, gate, and drain also the linear arrangement of the FET contacts is possible (fig. 3). In the linear geometry the clear gate acts as lateral termination of both the FET channel and the internal gate. The circular or ‘closed’ geometry has the inherent advantage of a ‘natural’ confinement of the internal gate by the negative potential of the surrounding drain region. For that reason it is the first choice for the XEUS WFI application. On the other hand the linear or ‘open’ geometry allows the design of smaller, more compact pixels. This quality makes DEPFET based pixel sensors of the linear design attractive for the use as vertex detectors in future linear colliders¹⁶. With the design rules of the current technology the minimum pixel size is 35 μm x 35 μm in the circular layout and 20 μm x 30 μm in the linear layout.

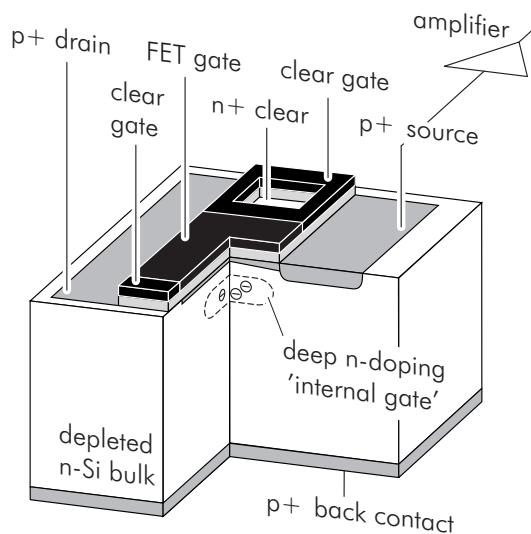


Figure 3

Section of a DEPFET in linear geometry. In integration the clear gate terminates both the transistor channel and the internal gate. The linear pixel geometry allows a minimum pixel size of 20 μm x 30 μm .

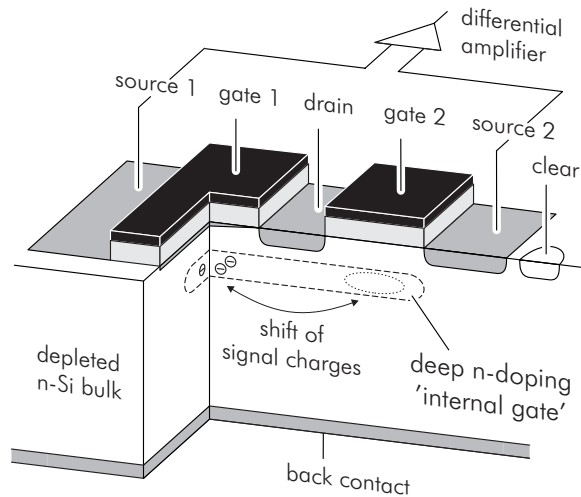


Figure 4

Section of a DEPFET for repetitive non-destructive readout. Two adjacent DEPFET devices in one pixel are able to transfer the signal charges from one internal gate to the neighboring one, reading the same signal information several times. The read noise is reduced by $n^{1/2}$, with n the number of readings.

4. REPETITIVE NON-DESTRUCTIVE READOUT

In a DEPFET the signal charges are strictly confined in a potential well. The information, i.e. the number of charges in the internal gate, is conserved throughout and after the readout procedure so that multiple reads of the same signal with subsequent averaging is possible. Repetitive readout results in a reduction of the $1/f$ noise contribution by $n^{1/2}$, with n the number of independent readings. The so-called Skipper CCD has already demonstrated that this technique allows spectroscopy measurements with sub-electron precision¹⁷.

The technique of repetitive non-destructive readout is best realized by the combination of two DEPFETs within one pixel and the lateral intra-pixel charge transfer between the two internal gates in a CCD-like mode. That way one of the DEPFETs reads the signal while the other one reads the baseline value of the empty internal gate. Moreover, connecting the signal lines of the two DEPFETs to the inputs of differential amplifier reduces the practical problem of common mode fluctuations. Figure 4 shows the possible layout of such a ‘ping pong’ DEPFET, in which the signal electrons are shifted across the common drain of the two transistors. Devices of this type have been fabricated and tests are under way.

5. ACTIVE PIXEL SENSOR

The matrix-like formation of DEPFETs with common back contact results in an Active Pixel Sensor (APS) with a unity fill factor. The thickness of the depleted bulk is 500 μm , giving high quantum efficiency at the high energy end of the XEUS energy range, e.g. 96% at 10 keV, 45% at 20 keV. Due to the total depletion of the bulk the DEPFET APS is illuminated through the uniform, non-structured backside. The low-energy response is given by the shallow p-implanted entrance window with an effective thickness smaller than 15 nm and an efficiency of 80 % at the C-K line (277 eV)^{18,19}. In addition the full depletion and backside illumination has a self-shielding effect: the radiation sensitive components of the DEPFET are placed on the non-irradiated surface and can only be hit by hard X-rays (> 10 keV), whose intensity is reduced by the absorption of the silicon bulk.

In its proposed layout the XEUS focal plane detector will be composed of 1024 x 1024 DEPFETs with a pixel size of 75 μm x 75 μm resulting in a total area of 7.68 cm x 7.68 cm integrated monolithically on a 6-inch wafer. Due to the diffusion-dominated extension of signal charge clouds along their drift to the internal gates, about 70% of the photons will hit more than one pixel. Therefore the coordinates of the photons’ interaction can be reconstructed by the centroid method with a precision considerably better than the pixel size. The position resolution is in any case better than 20 μm , and in the optimal case when the photon hits exactly the pixel border it is 4 μm . The energy of these split events can be reconstructed by pixel summation.

All DEPFETs in the pixel sensor have a common drain contact, while the gates, clear contacts, and clear gates are connected row-wise and the source contacts, i.e. the signal lines, are connected within each column. That way the pixel

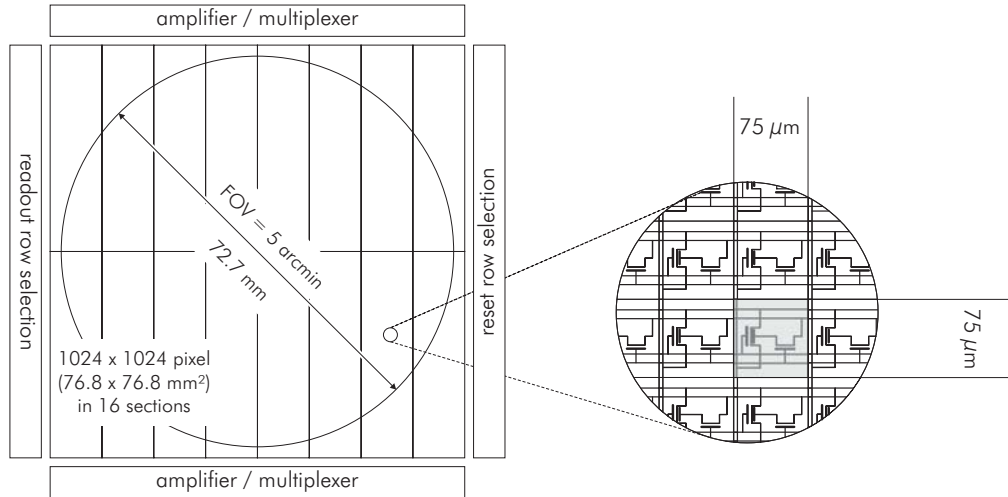


Figure 5

Layout of the Active Pixel Sensor for the XEUS Wide Field Imager focal plane. The 1024 x 1024 pixels are switched on and off for readout and reset row-wise by SWITCHER control electronics units at the left and right sides. The vertical channels of the APS are read out in parallel by CAMEX amplifier/multiplexer chips at the bottom and topside.

matrix is read and cleared row-wise, the readout of the DEPFETs in the selected row is done in parallel. The proposed APS for the XEUS Wide Field Imager consists of 16 sections each having a size of 128 x 512 pixels (fig. 5). This division into sections is purely logic, the full detector area is sensitive without any dead space between the subunits. All readout and reset operation steps mentioned above are applied to all sections simultaneously. To address one row of pixels for readout or reset control chips of the SWITCHER type²⁰ in a high-voltage CMOS technology are connected along the left and right sides to the matrix in fig. 5. From the left side one (horizontal) row of pixels is selected for readout. This is achieved by applying an appropriate gate voltage to all pixels of this row, which turns on the transistor currents. From the other side a clear pulse can be sent to a selected row. The control chips are identical, however a dedicated voltage supply and timing scheme has to account for either clearing or readout. The sections of the upper and lower detector halves are read out simultaneously in opposite directions. Each column, i.e. 512 pixels, of a section is fed into one channel of a DEPFET compatible preamplifier chip of the CAMEX type²¹.

As the individual pixels are random accessible, the APS has a high degree of flexibility in the choice of readout modes depending on the object and the scientific goal of an observation: In *full frame mode* the whole sensor area is read row by row. With the exception of one active row, all pixels are turned off and in integration mode, thus keeping dead time short and power consumption low. The processing time for one row is of the order of a few micro-seconds. The whole sensor is read within milli-seconds. In *window mode* only selected regions of interest that may have arbitrary rectangular shapes and sizes are read out, while the other pixels are suppressed. Time variations of fast transients will be observed in *timing mode*, i.e. a selected ROI is read at maximum speed but with reduced energy resolution. A limited area of 32 pixel rows or 2.5 mm in the readout direction could then be processed up to count rates of 10^5 sec^{-1} . Any combination of the above specified readout modes or *mixed mode* applied to dedicated regions of the sensor area is possible.

6. STATUS OF THE DEPFET APS

Recently a first series of APS prototypes for the XEUS application has been fabricated at the semiconductor laboratory of the Max-Planck-Institutes for physics and for extraterrestrial physics. It includes single DEPFET test structures and small pixel sensor arrays with a 64 x 64 format and 75 μm x 75 μm pixel size. For reasons of homogeneity and reproducibility in future large format pixel sensors the DEPFETs are of the MOS type. For the fabrication a new 6-inch technology for MOS devices on high resistivity substrates with two polysilicon layers and one metal layer has been

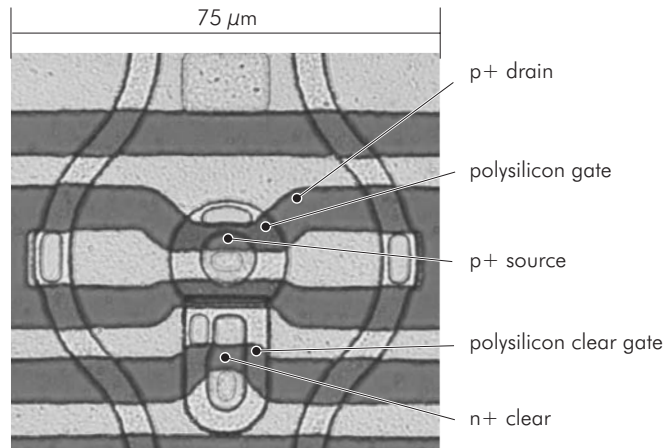


Figure 6

Microscope photography of a DEPFET pixel. The circular polysilicon gate has a width of 5 μm and a circumference of 40 μm. The bright horizontal lines are the metal connections of drain, gate, clear, and clear gate. The source is connected in vertical direction by the curved polysilicon lines.

developed. The process of a second metal layer, that is mandatory to avoid series resistance problems in large sensor arrays, is in progress.

Figure 6 is a microscope photograph of a circular DEPFET pixel as shown in figs. 1 and 2. The channel length, i.e. the width of the external polysilicon FET gate is 5 μm, the channel width, i.e. the mean gate circumference, is about 40 μm. Figure 7 shows a 16 x 12 pixel section of an APS with pads for the wire bond connections to the SWITCHER and CAMEX ASICs.

Isolated DEPFET pixels have been tested to proof the device principle and to obtain the performance parameters. Figure 8 shows an oscilloscope screenshot of the primary DEPFET signal, i.e. the drain current vs. time, obtained by a current/voltage converter circuit. The curve shows the slow linear increase of the drain current caused by the filling of the internal gate by thermally generated leakage current and the periodic reset by the clear pulse. The discrete steps in the curves are the response to signal charge packages generated by the absorption of X-ray photons arriving at the internal gate. At a given value the drain current saturates indicating that the internal gate is completely filled and no more able to store additional charges. The two photon events occurring right before the third clear pulse in fig. 8 demonstrate that the DEPFET also works as detector-amplifier in the case of internal gate saturation. Signal electrons arriving at the full internal gate induce a change of the drain current and discharge to the clear contact with a time constant of the order of 10 msec. In this mode the DEPFET works with dc-voltages only and can be used e.g. as readout device of Silicon Drift Detectors (SDDs)²².

The noise characteristics of single DEPFET devices have been evaluated by spectroscopic measurements. The DEPFET was configured in a source-follower circuit, and the data have been taken by a commercial spectroscopy system using a

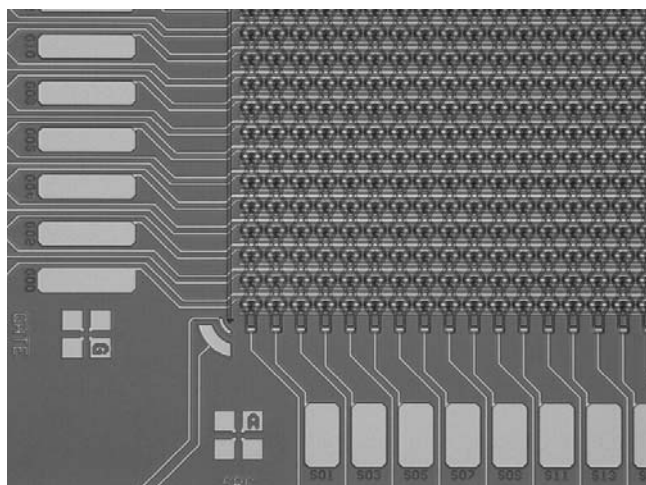


Figure 7

Microscope photography of a DEPFET pixel sensor. The bright metal rectangles are pads for the wire bond connections to the SWITCHER and to the CAMEX ASICs.

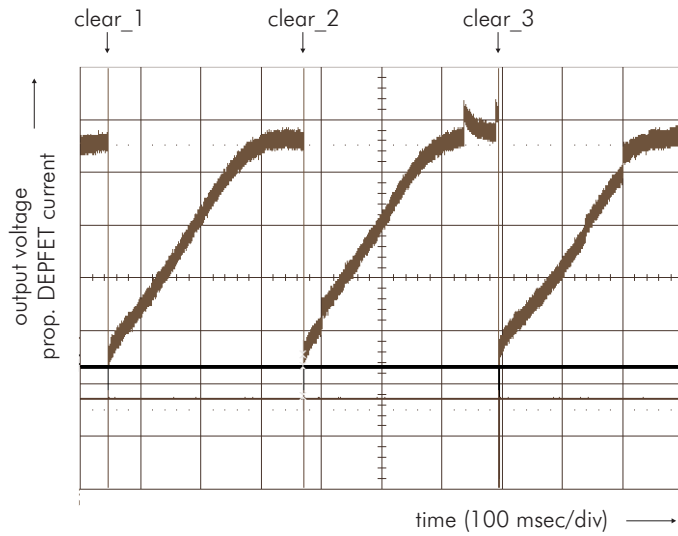


Figure 8

Oscilloscope screenshot of the primary DEPFET signal, i.e. drain current vs. time, obtained by a current/voltage converter circuit. The curve shows the slow linear increase of the drain current caused by the filling of the internal gate by thermally generated leakage current and the periodic reset by the clear pulse. The discrete steps in the curves are the response to signal charge packages generated by the absorption of X-ray photons arriving at the internal gate.

time-continuous filter with a shaping time constant of 6 μ sec. To simulate the conditions of pixel sensor readout the measurements have been made in the pulsed clear mode in a short time window after the clear pulse, i.e. with almost empty internal gate. Figure 9 shows the spectrum of a radioactive ^{55}Fe source with the Mn-K lines (5.9 keV, 6.5 keV) and the noise peak recorded at room temperature. The noise peak has been measured separately while the detector was not exposed to radiation. The width of the noise peak demonstrates an equivalent noise charge of only 2.2 el. rms at room temperature. In a single pixel measurement incomplete charge collection caused by charge splitting cannot be discriminated or corrected for. Therefore, the spectrum shows a pronounced low energy background, and the width of the Mn-K $_{\alpha}$ line is broadened to 131 eV FWHM by this effect as well. The operation of 64 x 64 pixel sensor systems including CAMEX readout and SWITCHER ASICs is in preparation.

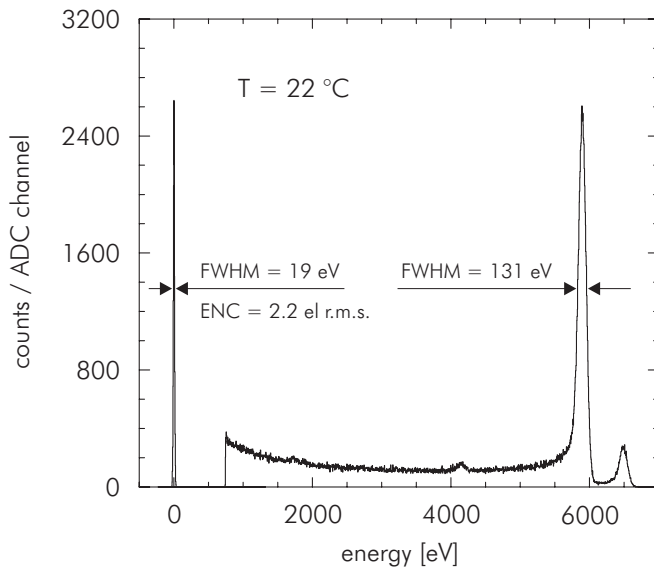


Figure 9

Spectrum of a ^{55}Fe source with the Mn K $_{\alpha}$ and Mn K $_{\beta}$ lines (5.9 keV, 6.5 keV) and the noise peak (0 eV) recorded with an isolated DEPFET pixel at room temperature. The noise in terms of equivalent noise charge is 2.2 el. rms. The low energy background is caused by charge splitting at the pixel borders.

ACKNOWLEDGEMENTS

The development of DEPFET pixel sensors and their readout and control systems profited from numerous fruitful discussions with our collaborators at the Universities of Bonn and Mannheim. The work on Active Pixel Sensors and related electronics for the XEUS Wide Field Imager was funded by ESA/ESTEC under the contract numbers 14897/00/NL/NB and 15851/01/NL/NB. The simulation software POSEIDON was developed by A. Castoldi, E. Gatti (Politecnico di Milano), and P. Rehak (Brookhaven National Laboratory) within the INFN-RIMAX project.

REFERENCES

1. The XEUS Astrophysics Working Group, "X-ray Evolving Universe Spectroscopy - The XEUS Science Case", *ESA SP-1238*, 2000
2. The XEUS Steering Committee, "X-ray Evolving Universe Spectroscopy - The XEUS Mission Summary", *ESA SP-1242*, 2000
3. The XEUS Telescope Working Group, "X-ray Evolving Universe Spectroscopy - The XEUS Telescope", *ESA SP-1253*, 2001
4. The XEUS Instrument Working Group, "X-ray Evolving Universe Spectroscopy - The XEUS Instruments", *ESA SP-1273*, 2003
5. ESA project "XMM", *ESA Bulletin 100* (special issue), 1999
6. S.L. O'Dell, M. Weisskopf, "Advanced X-ray Astrophysics Facility (AXAF)", *Proc. SPIE 3444*, p. 2, 1998
7. E. R. Fossum, "Are CCDs Dinosaurs?", *Proc. SPIE 1900*, p. 2, 1993
8. G. Prigozhin, S. Kissel, M. Bautz, C. Grant, B. LaMarr, R. Foster, G. Ricker, G. Garmire, "Radiation damage in the Chandra X-ray CCDs", *Proc. SPIE 4012*, p. 720, 2000
9. J. Kemmer, G. Lutz, "New detector concepts", *Nucl. Instr. and Meth. A 253*, p. 356, 1987
10. J. Kemmer, G. Lutz, U. Prechtel, K. Schuster, M. Sterzik, L. Strüder, T. Ziemann, "Experimental confirmation of a new semiconductor detector principle", *Nucl. Instr. and Meth. A 288*, p. 92, 1990
11. E. Gatti, P. Rehak, "Semiconductor drift chamber - an application of a novel charge transport scheme", *Nucl. Instr. and Meth. A 225*, p. 608, 1984
12. P. Klein, G. Cesura, P. Fischer, G. Lutz, W. Neeser, R.H. Richter, N. Wermes, "Study of a DEPFET Pixel Matrix with Continuous Clear Mechanism", *Nucl. Instr. and Meth. A 392*, p. 254, 1997
13. G.C. Holst, *CCD arrays, cameras, and displays*, JCD publishing & SPIE press, Bellingham, p. 109, 1996
14. A. Castoldi, E. Gatti, P. Rehak, "Three-Dimensional Analytical Solution of the Laplace Equation Suitable for Semiconductor Detector Design", *IEEE Trans. NS-43*, p. 256, 1996
15. A. Castoldi, E. Gatti, "Fast tools for 3-D design problems in semiconductor detectors", *Nucl. Instr. and Meth. A 377*, p. 381, 1996
16. R.H. Richter, L. Andricek, P. Fischer, K. Heinzinger, P. Lechner, G. Lutz, I. Peric, M. Reiche, G. Schaller, M. Schnecke, F. Schopper, H. Soltau, L. Strüder, J. Treis, M. Trimpl, J. Ulrici, N. Wermes, "Design and technology of DEPFET pixel sensors for linear collider applications", *Nucl. Instr. and Meth. A 511*, p. 250, 2003
17. R.P. Kraft, D.N. Burrows, G.P. Garmire, J.A. Nousek, J.R. Janesick, P.N. Vu, "Soft X-ray spectroscopy with sub-electron readnoise charge-coupled devices," *Nucl. Instr. and Meth. A 361*, p. 372, 1995
18. R. Hartmann, D. Hauff, P. Lechner, R. Richter, L. Strüder, J. Kemmer, S. Krisch, F. Scholze, G. Ulm, "Low energy response of silicon pn-junction detector", *Nucl. Instr. & Meth. A 377*, p. 191, 1996
19. R. Hartmann, L. Strüder, J. Kemmer, P. Lechner, O. Fries, E. Lorenz, R. Mirzoyan, "Ultrathin entrance windows for silicon drift detectors", *Nucl. Instr. and Meth. A 387*, p. 250, 1997
20. P. Klein, T. Aurisch, P. Buchholz, P. Fischer, M. Löcker, W. Neeser, L. Strüder, M. Trimpl, J. Ulrici, J. Vocht, N. Wermes, "A DEPFET Pixel Detector system for the use in Autoradiography", *Nucl. Instr. and Meth. A 454*, p. 152, 2000
21. W. Buttler, G. Lutz, V. Liberali, F. Maloberti, P.F. Manfredi, V. Re, V. Speziali, "Evolution in the criteria that underlie the design of a monolithic preamplifier system for microstrip detectors", *Nucl. Instr. and Meth. A 288*, p. 140, 1997
22. P. Lechner, S. Eckbauer, R. Hartmann, S. Krisch, D. Hauff, R. Richter, H. Soltau, L. Strüder, C. Fiorini, E. Gatti, A. Longoni, M. Sampietro, "Silicon drift detectors for high resolution room temperature X-ray spectroscopy", *Nucl. Instr. and Meth. A 377*, p. 346, 1996